Available online at www.sciencedirect.com
ScienceDirect
Journal of Power Sources 172 (2007) 14–19
JOURNAL OF POWER SOURCES
www.elsevier.com/locate/jpowsour

Short communication

Thermal studies of the state of water in proton conducting fuel cell membranes

T.L. Kalapos, B. Decker, H.A. Every, H. Ghassemi, T.A. Zawodzinski Jr. *

Department of Chemical Engineering and Case Advanced Power Institute, Case Western Reserve University, Cleveland, OH 44106, USA

Received 15 November 2006; received in revised form 19 April 2007; accepted 27 April 2007
Available online 6 May 2007

Abstract

The thermodynamics of acid group hydration was studied for different membranes (including Nafion® and sulfonated poly(arylene ether sulfone) (BPSH)) and model systems (including an organic/inorganic composite (I/O) and a multiblock polymer (MB-150)). Experiments were carried out with the membranes exposed to different activities of water corresponding to different levels of membrane hydration. Isopiestic sorption shows a significantly greater uptake in water for the multiblock polymer as compared to the others. Differential scanning calorimetry (DSC) was used to study thermal properties to elucidate the state of water in the membranes. A comparison is made of various modes of collecting data using DSC. Based on these data, we discuss the overall understanding of water interactions with these membranes as well as the limitations of thermodynamic data in describing microenvironments within the membrane.

Keywords: Fuel cell; Polymer electrolyte; Membrane; Isopiestic; DSC; Water

1. Introduction

In optimizing performance of polymer electrolyte fuel cell technology for applications, one must consider material performance in light of the entire fuel cell and power system. For example, though the optimal conditions for the present leading fuel cell membrane (i.e., Nafion®) are at full hydration and 80 °C, there are system advantages to operating at higher temperatures (>100 °C) and lower levels of hydration (∼25% relative humidity) in transportation applications. At higher temperatures, there is a greater driving force for heat rejection, requiring less exchanger surface area for heat removal. Raising the cell temperature can also significantly lower the poisoning affects of CO in certain hydrogen (reformate) feed streams by affecting the equilibrium constant for CO adsorption [1]. However, at temperatures approaching and greater than 100 °C (while maintaining atmospheric pressure), proton conductivity in polymer electrolyte membranes is typically lower than expected (based on thermal activation) [2] due to the accompanying decrease in water content.

Several aspects of the proton conduction mechanism are responsible for the decrease in conductivity. At higher water contents, the protons exhibit higher mobility, perhaps using a well-developed water network to 'hop' between neighboring water molecules in what is referred to as a Grotthuss mechanism [3]. On the other hand, at low water contents, proton conduction predominantly occurs via a vehicular mechanism—the protons and associated water move as a single entity [4]. This latter mechanism is a less effective means of proton transport, thus leading to a decrease in proton conductivity and corresponding decrease in cell performance. A higher water content is also desired as the presence of more water substantially screens the field associated with the negatively charged counterions, decreasing the 'restraining force' on protons and water, again enabling more facile transport.

Finally, in some cases the connectivity of the long-range conduction network may be improved by the swelling of the membrane that accompanies the higher water contents. Thus, the overall mobility of water and protons increases substantially with increasing water content. Though this increased mobility

* Corresponding author. Tel.: +1 216 368 5547; fax: +1 216 368 3016.
E-mail address: taz5@case.edu (T.A. Zawodzinski Jr.).

0378-7753/$ – see front matter © 2007 Elsevier B.V. All rights reserved.
doi:10.1016/j.jpowsour.2007.04.082

improves conductivity, it is a liability in direct methanol fuel cell (DMFC) operation where a high electro-osmotic drag of water in a swollen membrane can lead to greater methanol crossover. This motivates us to better understand and even tune the tightness of water binding in a fuel cell membrane.

The amount and properties of water present in the membrane are largely dependent on the nature of the interaction between the water and the ionic groups as well as on the mechanical properties of the polymer [5]. The latter is a key relevant parameter in determining the swelling of the polymer, while the former drives water uptake at relative humidity less than ∼75% [6].

Toward understanding the effects of water in the membrane, several workers have posited the existence of three 'states' of water in the membrane, corresponding to various non-freezing and freezing fractions of water as observed via DSC [7–12]. The freezing fraction of water is identified as loosely bound, or 'free' water and 'bound-freezable' water while the (non-observable) non-freezing fraction is identified with 'tightly bound' water. Similar distinctions have long been discussed in the context of porous media, such as porous glass and rocks and in the hydration of proteins [13,14]. In this mental construct, the transport properties of water and protons would be dependent on the population of the different environments.

While such a distinction may be a convenient mental picture, it has several limitations as a descriptive hypothesis. First, it is important to realize that the residence time of water in the various environments in a system at any temperature above the freezing point is such that only average properties of all water molecules are observed at timescales longer than a few tens of picoseconds. All *thermodynamic* or experimentally slow measurements then provide average values over all populations. Also, the inherent range of environments present in a polymer tends to blur any quantitative use of these distinctions. Nonetheless, the description of water in these environments is a qualitatively useful guide for broad correlations of properties. Our discussion in this context serves primarily as a caution to realize that the true situation represents a balance of different variables and that the existence of different micro-environments for water is more effect than cause.

It is the aim of this work to investigate and describe the thermodynamics of acid group hydration for different membranes and model systems. Isopiestic measurements were carried out with membranes that had been exposed to different activities of water corresponding to different levels of membrane hydration, providing access to free energy of water uptake. Differential scanning calorimetry (DSC) was performed with membranes that had been exposed to an activity of water of unity in order to examine the condition of water in the membranes, as either freezing or non-freezing. The enthalpic nature of the solvation interaction allows it to be readily characterized thermodynamically. This can be done through analysis of isopiestic data, i.e., the measurement of the sorption of water as a function of water activity in the vapor state, and, of course, using the DSC data.

2. Experimental

Nafion® 117 was obtained from Ion Power Inc. (Bear, Delaware). BPSH-35 membranes were synthesized in house according to the known procedure [15]. The membrane is a poly(arylene sulfone) polymerized from 3,3′-sulfonated and non-sulfonated 4,4′ dichlorodiphenylsulfone monomers with bisphenol A by a condensation reaction. The designation '35' refers to the percent sulfonation of the polymer. The multiblock polymer (MB-150) was synthesized in house by condensation polymerization of oligomeric blocks of BPSH-100 and oligomers formed from bisphenol A and decafluorobiphenyl according to a published procedure [16]. The structures of the BPSH and MB-150 polymers are shown in Fig. 1. The inorganic/organic composite membrane (I/O) was prepared by casting a composite film of poly(vinylidene difluoride) and silica particles that were surface modified with silylhexacanesulfonate from a dimethylacetamide solution. Surface modification of the silica was carried out by reacting silica particles with 11-bromo-undecyltrichoro silane in bicyclohexane at 80 °C for one day, followed by further reaction with potassium thioacetate in ethanol. The product was oxidized in a hydrogen peroxide/acetic acid mixture. Table 1 details the treating and cleaning procedures to yield the H^+ form of the membranes. After cleaning, and before equilibration, the membranes were stored immersed in DI water.

For isopiestic determinations, water uptake of the membranes was determined gravimetrically. First, the membranes

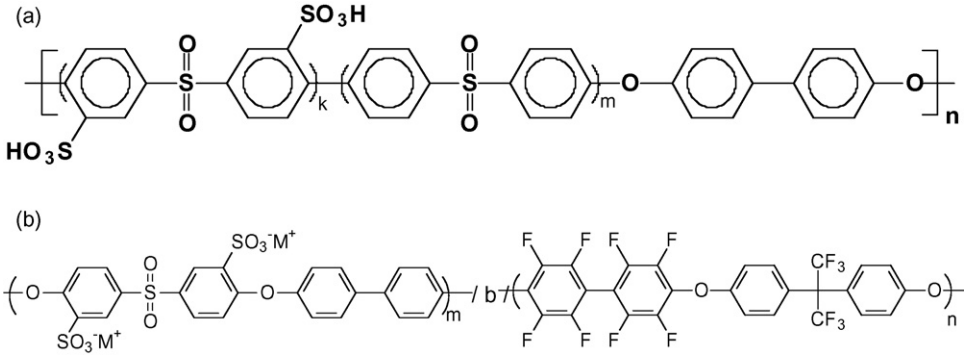

Fig. 1. Structures of: (a) BPSH-35 and (b) MB-150 used in this study.

Table 1
Membrane treatment

Membrane	Treating solution	Boiling time (h)
Nafion® 117	1.5% H_2O_2	1(1/2)
	Deionized water	1(1/2)
	0.5 M H_2SO_4	1(1/4)
	Deionized water	2
BPSH-35	0.5 M H_2SO_4	1(1/2)
	Deionized water	3
MB-150	0.5 M H_2SO_4	1
	Deionized water	1
Inorganic/organic	Deionized water	1(1/2)
	0.5 M H_2SO_4	1(1/2)
	Deionized water	3

were equilibrated at 30 °C in the vapor space of vials that contained solutions of LiCl that corresponded to specific activities of water vapor (a_w = 0.25, 0.75, 0.9, 1.0) and hence, different relative humidity values. The equilibrated samples were weighed and then dried in a vacuum oven and weighed again to determine the amount of water that was held at the respective humidity levels. Samples that were equilibrated under the same conditions, though not weighed nor dried, also were used for the DSC measurements.

Differential scanning calorimetry was performed with a Mettler Toledo DSC822e configured with an intra cooler capable of reaching temperatures of −70 °C. Sampling pans were 40 μl aluminum with pins on the bottom for consistent placement on the heating stage. Sample pan lids were either the standard type or those with a 50 μm pinhole that were found to allow a sufficient relief of pressure without prematurely drying out the membrane. More details are discussed below.

Before applying differential scanning calorimetry to water-saturated polymer membranes, scans were run with only water in the pan. This was to test the accuracy of the measurement of the specific heat of fusion and that of vaporization. In particular, there is a concern with using a hermetically sealed pan in the vaporization region of a volatile component, i.e., water. The concern is that the pan would pressurize and thereby elevate the boiling point and also at some point burst open and expel water mass and the heat content associated with it, thereby giving a false measurement of the specific heat of vaporization. To address this concern, we ran DSC of water in three pan configurations: (a) closed pan, (b) pan with a 50 μm pinhole in the lid and (c) open pan.

3. Results and discussion

3.1. Isopiestic sorption of water

Isopiestic sorption results obtained by equilibrating membrane samples at various water activities are shown in Fig. 2. The equilibrations were carried out to allow us to sample different water environments in our calorimetry experiments, i.e., to compare the DSC curves representing various amounts of water of solvation versus swelling. The isopiestic sorption results

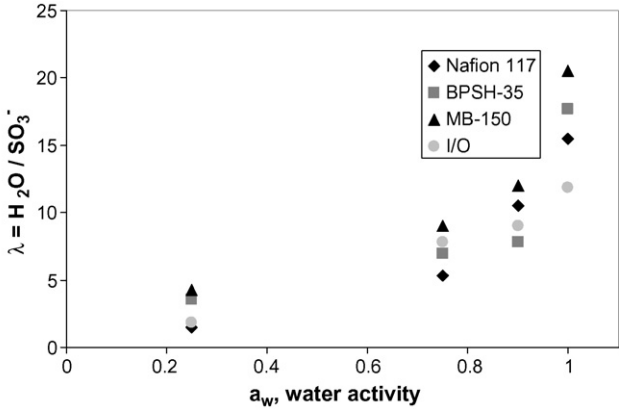

Fig. 2. Isopiestic sorption of vapor phase water (30 °C) showing the increase in water uptake with increased water activity.

show that membrane swelling at high relative humidity varies with polymer type, in the order MB-150 > BPSH-35 > Nafion® 117 > I/O. Though few points were taken in these studies, the isopiestic curves nonetheless exhibit the characteristic shape of such curves observed for ion exchangers in general. At low RH, relatively little uptake is observed. This region corresponds to the region of enthalpically driven solvation of acid groups of the polymer. Above ca. 75% RH, swelling of the polymer ensues.

Another useful analysis involves plotting $-\ln(a_w)$, which is directly related to the differential free energy of swelling of the polymer/water system, versus λ the number of water molecules per sulfonate group. The function $\ln a_w$ is the $\Delta(\Delta G_{sw})/RT$, where the activity is on the same basis as the reference for ΔG_{sw} and is simply obtained from the known thermodynamic properties of the equilibration solution. This plot, the differential of the isopiestic curve with axes swapped, indicates the free energy of uptake of water molecules per water molecule. As shown in Fig. 3, there is a significant decrease in the ordinate with respect to a small increase in λ. Beyond a range of λ from about 5 (for Nafion® 117) to 9 (for MB-150), the value of $-\ln(a_w)$ steadily approaches 0, indicating that there is little change in free energy beyond those values of λ. This implies that the majority of the

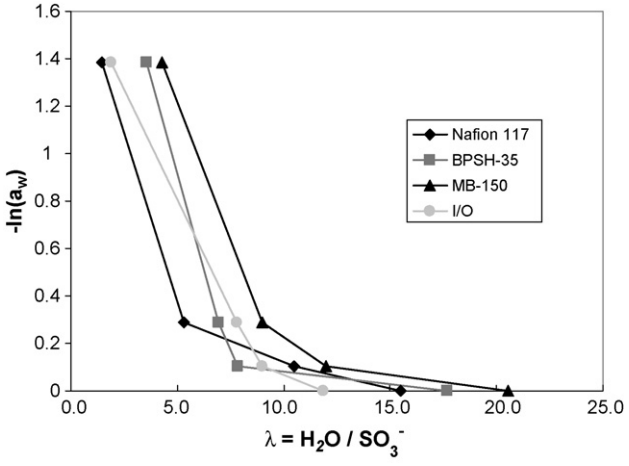

Fig. 3. Free energy of water uptake. Water is very weakly bound above λ ∼ 5 and increasingly tightly bound as λ decreases.

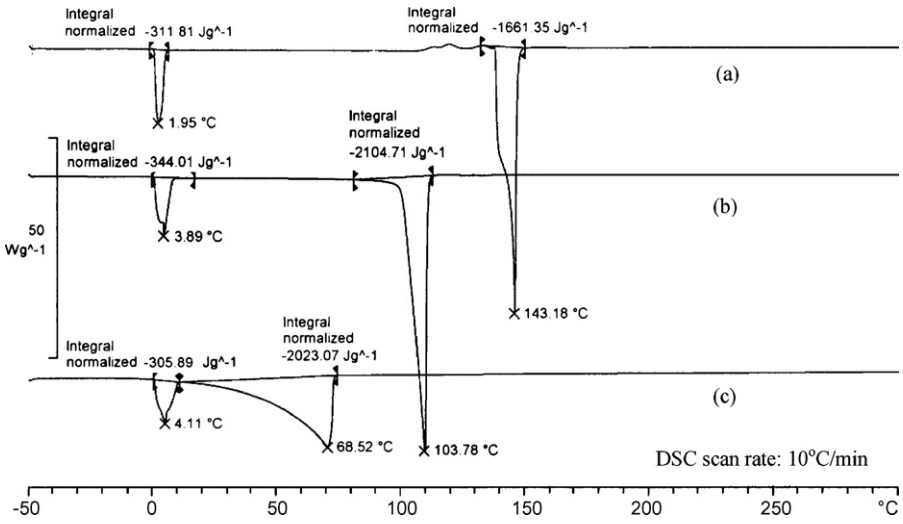

Fig. 4. DSC thermograms of water: (a) closed pan, (b) 50 μm pinhole and (c) open pan.

free energy change is associated with the ionizing and dissolving of protons by water on the sulfonic acid groups. Water is very weakly bound above $\lambda \sim 5$ or 6 and increasingly tightly bound as λ decreases. At high membrane water contents, there is a smaller driving force for additional water to absorb into the membrane. It is at these higher water contents that the membrane further expands (swells), thus forming the more extensive conduction networks for proton transport. Also at the higher water activities we can see different affinities that different membranes have for water which can provide insight into likely binding forces keeping H_2O in the membrane [17]. For example, the multi-block polymer (MB-150) consistently held more water per sulfonate group at a given water activity compared to the other membranes.

3.2. Differential scanning calorimetry

The results of the DSC scans with only water in the pan (Fig. 4) were as expected. All three pan configurations gave endotherms with integrated areas within 10% of the expected value for the specific heat of water fusion (333 J g^{-1}) with the biggest difference being with the open pan (8%), likely due to the sublimation of water into the DSC cell environment which did include a nitrogen purge. Greater differences were found in the vaporization region. The closed pan sample did show an elevated boiling point (peak of 143 °C) and a lower specific heat of vaporization (26% lower, based on the original amount of water in the pan) due to the loss of water upon the breaking of the pan seal. The pan with the 50 μm pinhole performed the best as it resulted in a smoother endotherm with a peak at 104 °C and a specific heat of vaporization within 7% of the expected value. The open pan configuration allowed the water to be gradually driven off even before reaching 70 °C, but could still account for approximately 90% of the expected specific heat of vaporization. These results gave us confidence to perform DSC with lids having the 50 μm pinhole.

For the analysis of DSC data for the subject membranes, we distinguish two temperature regions of interest, the 'water vaporization' region and the 'water melting' region.

3.3. Water vaporization region

Fig. 5 shows DSC thermograms of the tested membranes (−50 to 300 °C). In Table 2, results of the DSC studies of water vaporization from the membranes are summarized. An important aspect to note is the experimentally determined specific heat of vaporization of water (ΔH_v) from the membrane. In comparison to liquid water ($\Delta H_v = 2257$ J g^{-1}), the values for water vaporization from the membranes differ by only 3–11%. Broadly speaking, this tells us that the water expected to be in the membrane from the isopiestic measurements and subsequently expected to be driven off under the experimental conditions, is all accounted for. We cannot say with certainty whether differences in the observed value reflect real differences in enthalpy

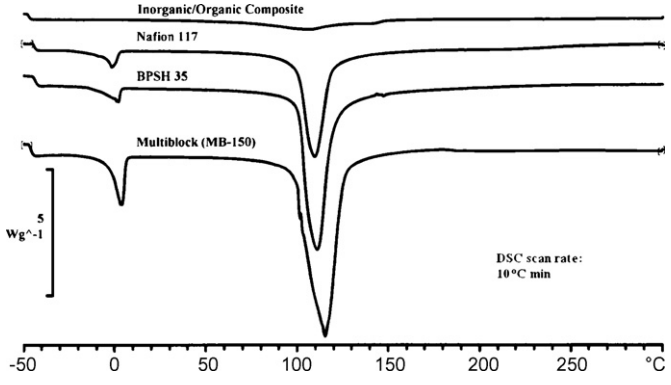

Fig. 5. DSC Thermograms of select membranes (−50 to 300 °C).

Table 2
Summary of DSC data for water vaporizing region

Sample	Water (wt%)	Endotherm peak (°C)	ΔH_v normalized (J g^{-1})	ΔH_v per mass water (J g^{-1} water)
Nafion®	19.9	112.1	435.6	2189
BPSH	32.8	109.5	710.9	2167
MB-150	35.7	114.5	864.4	2421
I/O	6.97	106.6	139.9	2007

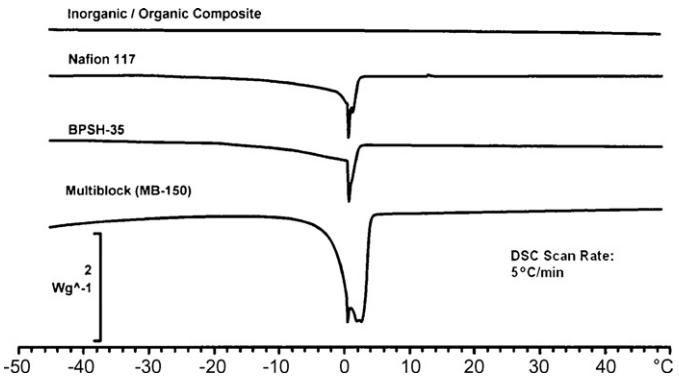

Fig. 6. Typical DSC thermograms of PEFC membranes in the water melting region. Here, MB-150 shows a significantly greater amount of 'freezable' water as compared to Nafion® 117 and BPSH-35.

of vaporization because of differences in the interaction strength or whether they are simply experimental error.

3.4. Water melting region

Fig. 6 shows the DSC thermograms of the tested membranes in the temperature range from −50 to 50 °C. There are generally two discernable peaks, one sharp and one rather broad and asymmetric, probably a composite of multiple smaller peaks. No attempt was made here to deconvolute the latter peaks. In Table 3, results of the DSC studies of water melting in the membranes are summarized. An important aspect to note here is the experimentally determined specific heat for the melting of water (ΔH_f). The comparison to liquid water ($\Delta H_f = 333\ J\ g^{-1}$) reveals significant deviations that can be interpreted in several different ways. First, the mean heat of fusion of water in the membrane could be different from that of liquid water, indicating stronger or weaker enthalpies of interaction between water and the membrane/water system than the enthalpy of interaction of water in water. A second interpretation is that not all of the water present was frozen, even at −50 °C, the beginning of the DSC scan, indicating stronger enthalpies of interaction. In this second case, the entire mass of water cannot be divided into the total amount of heat represented by the melting endotherm. Finally, the amount of water expected to be present could be incorrectly stated.

The third interpretation is refuted, within experimental error, when we consider that the expected amount of water is entirely revealed in the vaporization region, and therefore, would have also been present in the melting region. This leaves us with the possibilities of: (1) lower molar enthalpy of water fusion and (2) the presence of non-freezing water, either of which could be due to interactions of water with the membrane. The second hypothesis tacitly assumes that the heat of fusion of water in the membrane is unchanged from that of the liquid. The validity of this assumption is of some concern. However, from these data, it is not possible to distinguish between these possibilities, and thus *it is difficult to state quantitatively, from this data alone, how much 'bound, freezable' water exists in the membrane*.

In fact, at water contents below complete saturation, there is generally not much direct evidence in the DSC data for a 'freezing' fraction of water at any water content below the highest hydration levels [18]. In fairness to the authors of ref. [18], additional information beyond the DSC results is brought to bear on the question. However, this relies on treating 'non-freezing' water as a component in a polymer blend and deducing the amount of non-freezing water from the shift in apparent T_g. The correlation used is an empirical rule of thumb that approximates the glass transition temperature of a polymer blend from the individual T_g's of the component polymers. One could question the applicability of this assumption to the case of water as a blending component, especially given the completely empirical nature of the correlation.

In ref. [18], DSC plots at λ values lower than ∼12 show no sharp freezing peak. The absence of additional peaks in the water-melting region, in conjunction with the low heat of melting and normal heat of vaporization, is generally interpreted as indicating that the water is 'non-freezing'. From the isopiestic data, water does indeed interact strongly with the membrane at low relative humidity or water content. However, water sorbed into the membrane in the 'swelling' region (above ∼6 waters per sulfonic acid) also does not contribute a freezing peak in many cases, even though its interaction with the membrane is not strong (see the $\ln(a_w)$ versus λ plot). The fraction of water that is in this intermediate zone would correspond to the 'bound, freezable' water. However, if, as is typical, the freezing fraction is identified with 'bulk-like' water similar to liquid water and the non-freezing fraction is identified as 'bound water', it seems logical to expect all weakly interacting water to contribute to the 'freezing' peak. Yet, by comparing isopiestic and DSC data we find that a substantial fraction of the water is both weakly interacting and apparently non-freezing in the DSC sense. Because of the ambiguity regarding the amount of water in the intermediate state, we are unsure of the strength of the correlation between amount of freezable, loosely bound water and transport properties, such as those in ref. [18].

One also wonders about the relevance of the bulk/bound distinction to other transport properties. If the free water state is somehow critical to transport, we should see sharp transitions

Table 3
Summary of DSC data for water melting region

Sample	Water (wt%)	Melting peak (°C)	ΔH_f normalized ($J\ g^{-1}$ sample)	ΔH_f per mass water ($J\ g^{-1}$ water)	Freezing water (λ)	Non-freezing water (λ)
Nafion®-117	19.9	−0.41	35.21	176.9	8.3	7.2
BPSH-35	32.8	0.36	32.53	99.2	5.3	12.4
MB-150	35.7	3.71	84.07	235.5	14.6	6
I/O	6.97	None	–	–	–	11.9

in properties due to its presence. Freezing or free water is only present at very high water contents, with little to conclude from DSC regarding water much below $a_w \sim 1$. However, the primary sharp transition in conductivity as a function of water content occurs below $\lambda \sim 6$ waters per sulfonate, the point at which the water becomes primarily associated with solvation of the fixed acid sites. This is clearly highlighted in isopiestic curves, but not in DSC. This regime may be key for conduction at operating temperatures of 120 °C, when only the tightly held water may be present in the membrane.

On the other hand, weakly bound, bulk-like water as well as 'bound, freezable' are likely to be an important contributor to electro-osmosis, and indeed the drag coefficient apparently sharply rises as the membrane is exposed to liquid water, i.e., when the bulk water is high. This aspect is clearly shown by DSC. Another way of looking at this is to consider the weakness of water binding, revealed directly by the isopiestic curve, and regard the observed electro-osmotic drag coefficient as reflecting a balance between the force holding water in place versus that arising from the field associated with a moving proton. This latter picture will be more fully explored elsewhere [19].

4. Conclusions

In summary, isopiestic and DSC data provide complementary information on the thermodynamics of water sorption in proton conducting membranes. We support the use of 'pressurized' DSC for accurate and reproducible studies of water in polymer electrolytes. Based on our discussion of the data, we raise a cautionary note regarding interpretation of transport data based on simple pictures of water/membrane interactions, especially those based solely on DSC data.

Acknowledgements

We gratefully acknowledge the financial support of the United States Department of Energy OHFCIT for this research. The authors also recognize the contributions of other members of the CAPI lab, especially Derek Lebzelter.

References

[1] T. Springer, T. Zawodzinski, S. Gottesfeld, in: J. McBreen, S. Mukherjee, S. Srinivasan (Eds.), PV 97-13, The Electrochemical Society Proceedings Series, Pennington, NJ, 1997, pp. 15–24.
[2] T.A. Zawodzinski Jr., C. Derouin, S. Radzinski, R.J. Sherman, T. Springer, S. Gottesfeld, J. Electrochem. Soc. 140 (1041) (1993).
[3] C.J.D. van Grotthuss, Ann. Chim. 58 (1806) 54.
[4] K.D. Kreuer, W. Weppner, A. Rabenau, Angew. Chem., Int. Ed. Engl. 21 (1982) 208.
[5] S. Gottesfeld, T.A. Zawodzinski, in: R.C. Alkire, H. Gerischer, D.M. Kolb, C.W. Tobias (Eds.), Advances in Electrochemical Science and Engineering, Wiley-VCH, Weinheim (Germany), 1997, p. 251.
[6] S. Gottesfeld, T.A. Zawodzinski, in: R.C. Alkire, H. Gerischer, D.M. Kolb, C.W. Tobias (Eds.), Advances in Electrochemical Science and Engineering/1997, Wiley-VCH, Weinheim (Germany), 1997, pp. 253–254.
[7] M. Escoubes, M. Pineri, in: A. Eisenberg, H.L. Yaeger (Eds.), Perfluorinated Ionomer Membranes, American Chemical Society, Washington, DC, 1982, pp. 16–23.
[8] R.M. Hodge, G.H. Edward, G.P. Simon, Polymer 37 (1996) 1371.
[9] G. Xie, T. Okada, Deni Kagaku 64 (1996) 718.
[10] W.G. Liu, K.D. Yao, Polymer 42 (2001) 3943.
[11] T. Takei, K. Kurosaki, Y. Nishimoto, Y. Sugitani, Anal. Sci. 18 (2002) 681.
[12] Y.S. Kim, L. Dong, M.A. Hickner, T.E. Glass, V. Webb, J.E. McGrath, Macromolecules 36 (2003) 6281.
[13] S. Stapf, R. Kimmich, J. Chem. Phys. 103 (1995) 2247.
[14] I.D. Kuntz, W. Kauzmann, Adv. Protein Chem. 28 (1974) 239.
[15] F. Wang, M. Hickner, Y.S. Kim, T.A. Zawodzinski, J.E. McGrath, J. Membr. Sci. 197 (2002) 231.
[16] H. Ghassemi, W. Harrison, T.A. Zawodzinski Jr., J. E. McGrath, Polymer Preprints, American Chemical Society, Division of Polymer Chemistry, vol. 45, 2004, p. 68.
[17] D.R. Lebzelter, Characterization of fuel cell transport properties in sulfonated poly(arylene ether sulfone) membranes, Master's Thesis, Case Western Reserve University, Cleveland, 2004.
[18] Y.S. Kim, L. Dong, M. Hickner, T.E. Glass, J.E. McGrath, Macromolecules 36 (17) (2003) 6281–6685.
[19] Y. Wu, H. Every, T.A. Zawodzinski Jr., in preparation.